



# Development of voxel-based optimization diffusion kurtosis imaging (DKI) and comparison with conventional DKI

Masanori Maehara<sup>1</sup>

Received: 26 September 2018 / Revised: 25 June 2019 / Accepted: 26 June 2019 / Published online: 5 July 2019  
© Japanese Society of Radiological Technology and Japan Society of Medical Physics 2019

## Abstract

The aims of this study were to implement voxel-based optimization diffusion kurtosis imaging (DKI) and evaluate the accuracy of the method for the analysis of diffusion imaging data in comparison with conventional DKI. Conventional DKI and voxel-based optimization DKI were tested on a phantom and a human in a 1.5 T whole-body scanner. The differences in the diffusion coefficient ( $D$ ) and diffusion kurtosis ( $K$ ) values were analyzed using the Mann–Whitney  $U$  test, and the Holm correction was applied to the statistical analyses. In the phantom study, the  $D$  value resulting from voxel-based optimization DKI was significantly lower than those from conventional DKI in water and agarose solutions at concentrations of 50 and 100 g/L (all  $p < 0.01$ ). Moreover, the  $K$  value was significantly lower in the water and agarose solutions at concentrations of 50, 100, and 200 g/L (all  $p < 0.01$ ). In the human study, the  $D$  value resulting from voxel-based optimization DKI was significantly lower than that of conventional DKI in both white matter (WM), and gray matter (GM) (all  $p < 0.01$ ). Moreover, the  $K$  value was significantly lower in cerebrospinal fluid, WM, and GM (all  $p < 0.01$ ). To correctly measure the DKI, the optimized  $b$  values for each voxel must be used. Voxel-based optimization DKI is a method that optimizes the  $b$  values for each voxel. It appears that voxel-based optimization DKI improves the accuracy of the  $K$  value for biological tissues.

**Keywords** DKI · Kurtosis · Diffusion kurtosis imaging

## 1 Introduction

Diffusion weighted imaging (DWI) is widely applied as a noninvasive magnetic resonance imaging (MRI) method that provides an image contrast based on the molecular motion of water. Because structural changes to biological tissues alter their diffusion coefficient, DWI provides a sensitive measure of structural information in biological tissues. Previous reports have shown the utility of applying DWI in various regions of the body [1–4].

The diffusion of water through biological tissues can be regarded as a random process. The degree to which a particular water molecule diffuses from one location to another within a given period of time is governed by a probability distribution. In the simplest diffusion models, this distribution is based on the assumption that the spatial distribution

profile of the diffusion of water molecules is Gaussian. However, for time intervals on the order of tens of milliseconds, particularly in the complex environmental structure of most tissues, which consist of various types of cells and their membranes, the spatial distribution profile of the diffusion of water molecules cannot be fully described as a simple change by the Gaussian assumption [5]. Such non-Gaussianity is called diffusion kurtosis, which can be quantified based on the tissue structure, because a deviation from a Gaussian form is governed by the complexity of the tissue within which the water is diffusing.

The diffusion kurtosis imaging (DKI) analysis technique proposed by Jensen requires the use of images with multiple  $b$  values, including high  $b$  values, to calculate the diffusion kurtosis. The parametric maps of the diffusion coefficient ( $D$ ) value, which is an estimate of the diffusion coefficient in the direction parallel to the orientation of a diffusion sensitizing gradient, called a motion probing gradient (MPG), and of the diffusion kurtosis ( $K$ ) value, which is an estimate of the diffusion kurtosis in this same direction, are created by fitting the DWI data of multiple  $b$  values for each voxel to the following formula:

✉ Masanori Maehara  
masanori.maehara@gmail.com

<sup>1</sup> Department of Radiology, Nihon University School of Dentistry at Matsudo, 2-870-1, Sakae-nishi, Matsudo 271-8587, Chiba, Japan

$$S_{\text{exp}} = S_0 \exp\left(-bD + \frac{1}{6}b^2D^2K\right), \quad (1)$$

where  $S_{\text{exp}}$  is the experimental signal intensity,  $S_0$  is the signal intensity without MPGs, and  $b$  is the  $b$  value, which is usually given by the expression  $b = (\gamma\delta g)^2(\Delta - \delta/3)$ , where  $\gamma$  is the proton gyromagnetic ratio,  $\delta$  is the duration of the MPG,  $g$  is the strength of the MPG, and  $\Delta$  is a time interval between the centers of the MPGs [6, 7]. Jensen reported that the maximum  $b$  value for DKI should be carefully chosen. For DKI of the brain, empirical evidence indicates that a maximum  $b$  value of 2000–3000 s/mm<sup>2</sup> is appropriate [7]. In addition, based on a previous report, the DKI should be measured using the optimized  $b$  values to calculate the correct diffusion kurtosis [8]. The optimal  $b$  values used to calculate the correct diffusion kurtosis are different for each voxel because the diffusion behavior is different for each voxel. Therefore, the aims of this study were to implement voxel-based optimization DKI to measure the correct diffusion kurtosis using optimized  $b$  values for each voxel and compare the method with conventional DKI for the case of the human brain.

## 2 Materials and methods

Conventional DKI and voxel-based optimization DKI were tested on a phantom and a human in a 1.5 T whole-body scanner (Intera Achieva 1.5 T Nova, Philips, Netherlands) using a maximum gradient strength of 66 mT/m and a gradient slew rate of 160 mT/m/ms with a Philips 8-channel SENSE head coil.

Parametric maps of the  $D$  and  $K$  values were obtained by fitting the image signal intensities in a pixel-wise manner using the nonlinear least-squares method in MATLAB R2014b (MathWorks, USA). Conventional DKI was implemented by fitting the DWI data to formula (1).

A statistical analysis of the data was conducted using R software (version 3.4.3; R Project for Statistical Computing, Vienna, Austria). The differences in  $D$  and  $K$  values between conventional DKI and voxel-based optimization DKI were analyzed using the Mann–Whitney  $U$  test, and the Holm correction was applied to the statistical analyses. A value of  $p < 0.05$  was considered to indicate a statistically significant difference. Data were presented as mean  $\pm$  SD.

### 2.1 Voxel-based optimization DKI analysis

To calculate the correct  $D$  and  $K$  values, a voxel-based optimization DKI analysis requires greater use of the images of multiple  $b$  values than a conventional DKI analysis, as reported by Jensen. The combination used in this study for the voxel-based optimization DKI analysis included multiple  $b$  values of 0, 500, 1000, 1500, 2000, and 3000 s/mm<sup>2</sup>. The

following algorithm is illustrated as a flow chart in Fig. 1. There are two steps in the post-processing procedure for the voxel-based optimization DKI. The first step is to remove data whose noise level may affect the accuracy of the diffusion kurtosis. Data whose signal intensity decrease by 5% relative to data with a  $b$  value of 0 s/mm<sup>2</sup> are regarded as noise. In the second step, if there are fewer than three DWI data points after the first step, assuming that the water diffusion exhibits Gaussian behavior ( $K$  value = 0), the  $D$  value is calculated by fitting the DWI data to the following formula:

$$S_{\text{exp}} = S_0 \exp(-bD). \quad (2)$$

If there are exactly three DWI data points, the  $D$  and  $K$  values are calculated by fitting the DWI data to the following formula:

$$\log S_{\text{exp}} = -bD + \frac{1}{6}b^2D^2K + \log S_0. \quad (3)$$

If there are more than three DWI data points,  $D$ ,  $K$ , and  $S_0'$  are calculated by fitting the DWI data without a  $b$  value of 0 s/mm<sup>2</sup> to the following formula:

$$\log S_{\text{exp}} = -bD + \frac{1}{6}b^2D^2K + \log S_0', \quad (4)$$

where  $S_0'$  is the simulated signal intensity at  $b = 0$  s/mm<sup>2</sup>. Using  $S_0'$  instead of  $S_0$  and DWI data points with  $b$  values of 500 s/mm<sup>2</sup> or more, the parametric maps of the  $D$  and  $K$  values should theoretically be unaffected by perfusion because data with  $b$  values of less than 100–200 s/mm<sup>2</sup> reflect the influence of perfusion, whereas data with  $b$  values of 500 s/mm<sup>2</sup> or greater reflect the influence of diffusion [4, 9]. Thus, these steps should reliably obtain the diffusion kurtosis more correctly than conventional DKI because they remove background noise and the influence of perfusion.

### 2.2 Phantom study

To compare the  $D$  and  $K$  values from conventional DKI to the voxel-based optimization DKI resulting from the standard DWI as described above, the DWI was applied to a multi-compartment phantom. The phantom consisted of five cylindrical sample bottles filled with water; agarose solutions at concentrations of 50, 100, and 200 g/L; and asparagus to simulate biological tissues with a nonzero kurtosis.

The imaging parameters for the acquisition were as follows: a repetition time (TR) of 5000 ms, an echo time (TE) of 92 ms, a field of view (FOV) of 250 mm  $\times$  225 mm, an acquisition matrix of 128  $\times$  102, an acquisition pixel size of 1.95 mm  $\times$  2.47 mm, a recon matrix of 256  $\times$  256, a recon pixel size of 0.98 mm  $\times$  0.98 mm, and 15 slices, each with a thickness of 5 mm. Conventional DKI and voxel-based optimization DKI were performed using six  $b$  values (0, 500, 1000, 1500, 2000, and 3000 s/mm<sup>2</sup>) and the average of

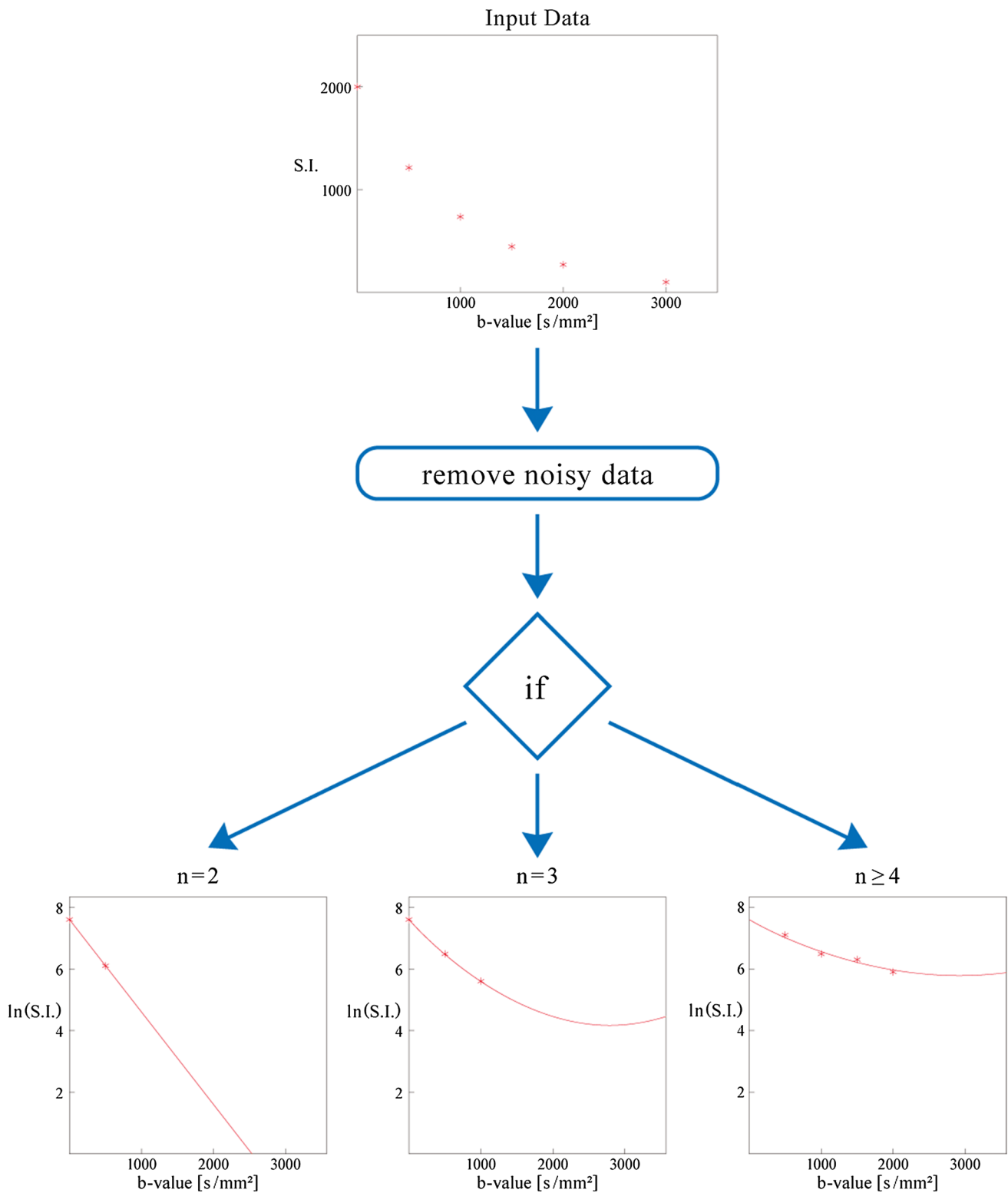


**Fig. 1** Flow chart of the proposed algorithm for voxel-based optimization DKI. The first step is the removal of noisy data. Data points whose signal intensity decreases by 5% relative to data with a  $b$  value

of 0  $\text{s/mm}^2$  are regarded as noise. The second step is fitting the data to formula (2) (3), or (4) based on the number of non-noisy data points.  $n$  is number of data

six MPG directions. Three values of the number of signals averaged (NSA) were used: 1 ( $b = 0$ ), 2 ( $b = 500$ ), and 3 ( $b \geq 1000$ ). The acquisition time for a voxel-based optimization DKI sequence was 7 min. The phantom was scanned ten times. Each measurement was performed using a circular region of interest (ROI) comprising 15 pixels ( $\phi$ ), and the average values were used for comparison.

### 2.3 Human study

The human study was conducted on a single healthy volunteer using conventional DKI and voxel-based optimization DKI after obtaining their informed consent, as required by the institutional review board.

The parameters for the conventional DKI and voxel-based optimization DKI chosen for this study were the same as those used in the phantom study. The  $D$  and  $K$  values of the cerebrospinal fluid (CSF), white matter (WM), and gray matter (GM) of the healthy volunteer were compared with those obtained using conventional DKI and voxel-based optimization DKI. The volunteer was scanned ten times. Each measurement was performed using the widest settable circular or freehand ROI, as shown in Fig. 2, and the average values were used for comparison.

## 3 Results

### 3.1 Phantom study

Parametric maps of  $D$  and  $K$  values were created in the multi-compartment phantom using data acquired from

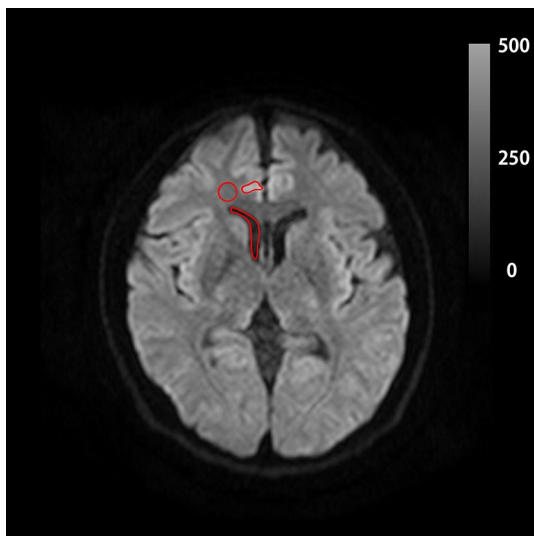


**Fig. 2** DWI with  $b$  value of  $1000 \text{ s/mm}^2$ . The  $D$  and  $K$  values of the CSF, WM, and GM of the healthy volunteer were measured using circular or freehand ROI

both conventional DKI and voxel-based optimization DKI (Fig. 3). The locations “bottle 1”, “bottle 2”, “bottle 3”, “bottle 4”, and “bottle 5” refer to those in Fig. 3 and correspond to water; agarose solutions at concentrations of 50, 100, and 200 g/L; and asparagus, respectively. Moreover, Fig. 4 depicts a comparison of the  $D$  and  $K$  values resulting from both conventional DKI and voxel-based optimization DKI.

The  $D$  value resulting from voxel-based optimization DKI was significantly lower than those of conventional DKI in water and agarose solutions at concentrations of 50 and 100 g/L (all  $p < 0.01$ ). Moreover, the  $K$  value was significantly lower in the water and agarose solutions at concentrations of 50, 100, and 200 g/L (all  $p < 0.01$ ).

### 3.2 Human study

Parametric maps of the  $D$  and  $K$  values were created from a healthy volunteer using both conventional DKI and voxel-based optimization DKI (Fig. 5). The parametric maps from the two techniques are compared in Fig. 6 for ROIs in the CSF, WM, and GM.

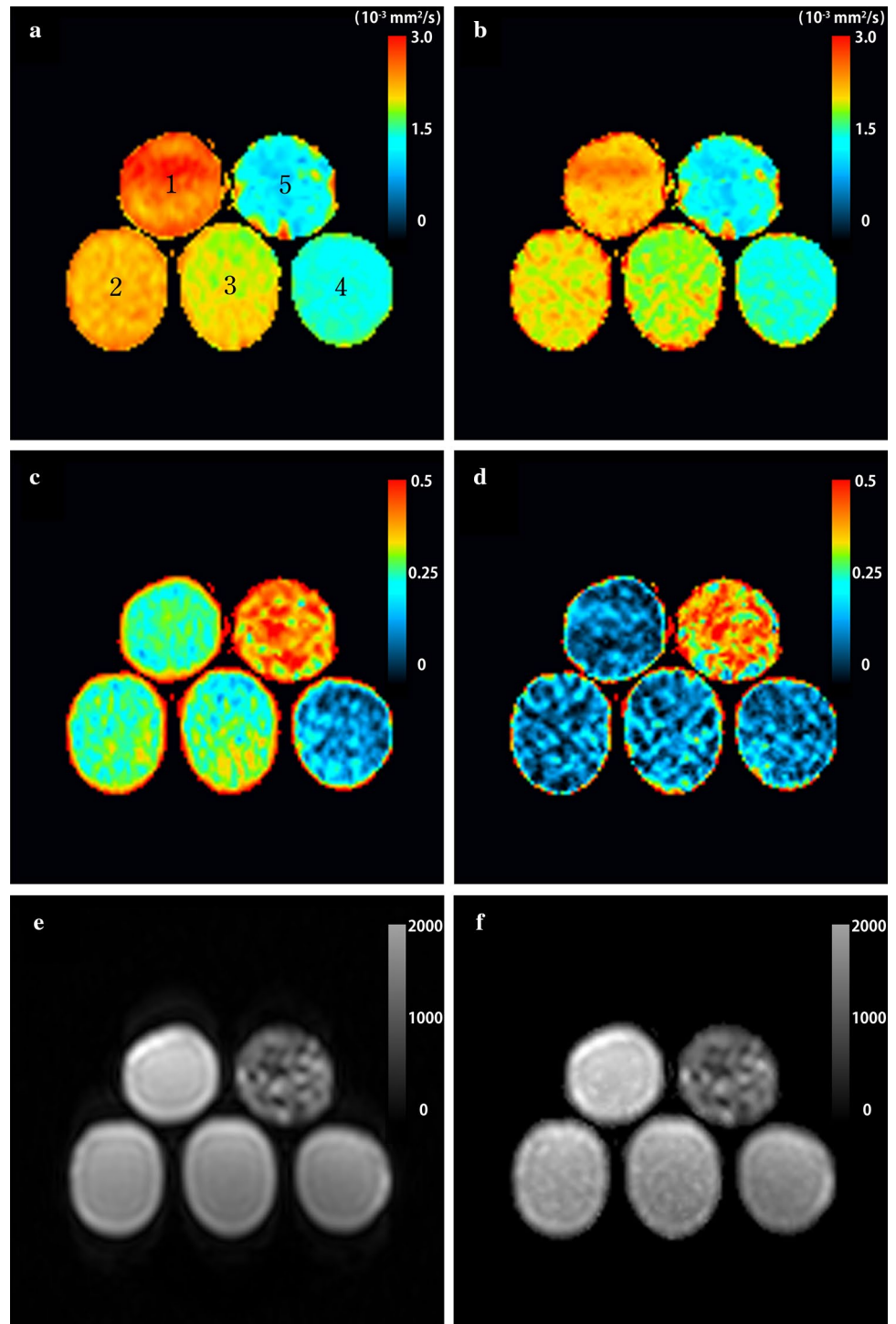
The  $D$  value resulting from voxel-based optimization DKI was significantly lower than that of conventional DKI in the WM and GM (all  $p < 0.01$ ). Moreover, the  $K$  value was significantly lower in the CSF, WM, and GM (all  $p < 0.01$ ).

## 4 Discussion

In the complex environment of biological tissues, influence of the tissue microstructure on water diffusion cannot be fully described as a simple change in Gaussian form. Thus, the DKI, which can quantify the deviation from a Gaussian behavior, is helpful in detecting microstructural changes in the tissue. However, the DWI data used to calculate the diffusion kurtosis are affected by background noise and tissue perfusion, the degrees of which are different for each voxel. Thus, the DKI needs to be correctly measured using the optimized  $b$  values for each voxel. The voxel-based optimization DKI described in this study is a method for optimizing the  $b$  values for each voxel. This method was applied using a maximum  $b$  value of  $3000 \text{ s/mm}^2$  based on the fact that Lu et al. showed that the quadratic approximation is invalid beyond this value [10]. Moreover, the point of intersection of the fast and slow components of bi-exponential decay is called the fractional  $b$  value, and Ogura et al. reported that the fractional  $b$  value of normal WM, GM, and the thalamus was  $1700 \text{ mm}^2/\text{s}$ , though the values in other organs may be different [11, 12].

In the phantom study, the  $D$  and  $K$  values resulting from voxel-based optimization DKI were significantly lower

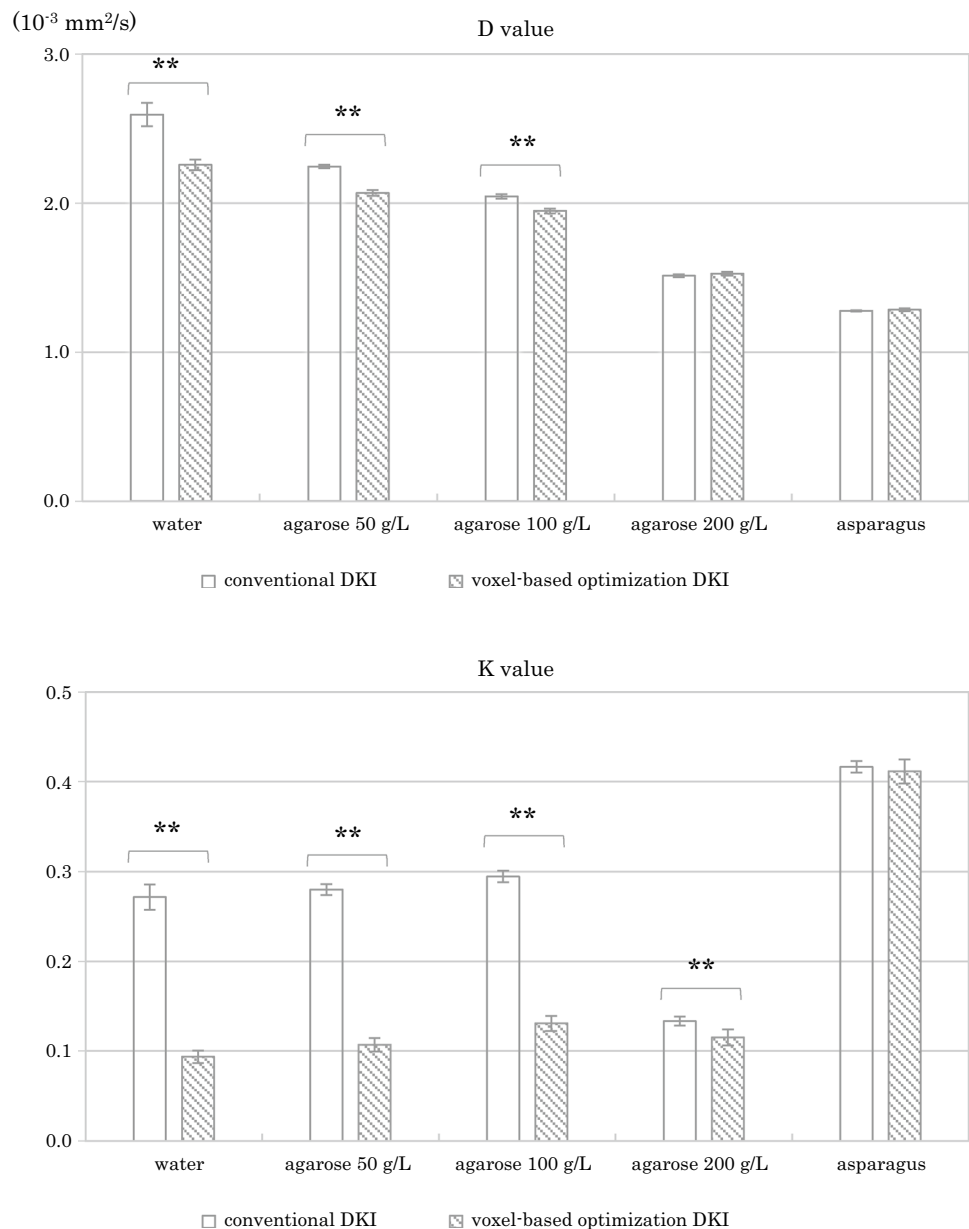
**Fig. 3** Parametric maps of  $D$  and  $K$  values in multi-compartment phantom using data obtained from conventional and voxel-based optimization DKI: **a**  $D$  value with conventional DKI, **b**  $D$  value with voxel-based optimization DKI, **c**  $K$  value with conventional DKI, **d**  $K$  value with voxel-based optimization DKI, **e** image with  $b$  value of 0 s/mm<sup>2</sup>, and **f**  $S_0'$  with voxel-based optimization DKI. The locations of bottles 1, 2, 3, 4, and 5 correspond to water; agarose solutions at concentrations of 50, 100, and 200 g/L; and asparagus, respectively



than those from the conventional DKI in water and agarose solution. In particular, the  $K$  value obtained using voxel-based optimization DKI was considerably lower. This is because noisy data were removed by the first step of the technique. Jensen et al. reported that the mean diffusion kurtosis value in freely diffusing water molecules is theoretically zero [6].

In the human study, the  $D$  and  $K$  values resulting from voxel-based optimization DKI were significantly lower than those from the conventional DKI in CSF for the same reason as the water and agarose in the phantom study. The  $K$  value obtained using voxel-based optimization DKI was significantly lower, like that of the water and agarose solution in the phantom study. Yang et al. reported that the  $K$

**Fig. 4** Comparison of  $D$  and  $K$  values resulting from conventional and voxel-based optimization DKI for multi-compartment phantom. Statistically significant differences with  $p < 0.05$  are marked with single asterisk and statistically significant differences with  $p < 0.01$  are marked with double asterisks

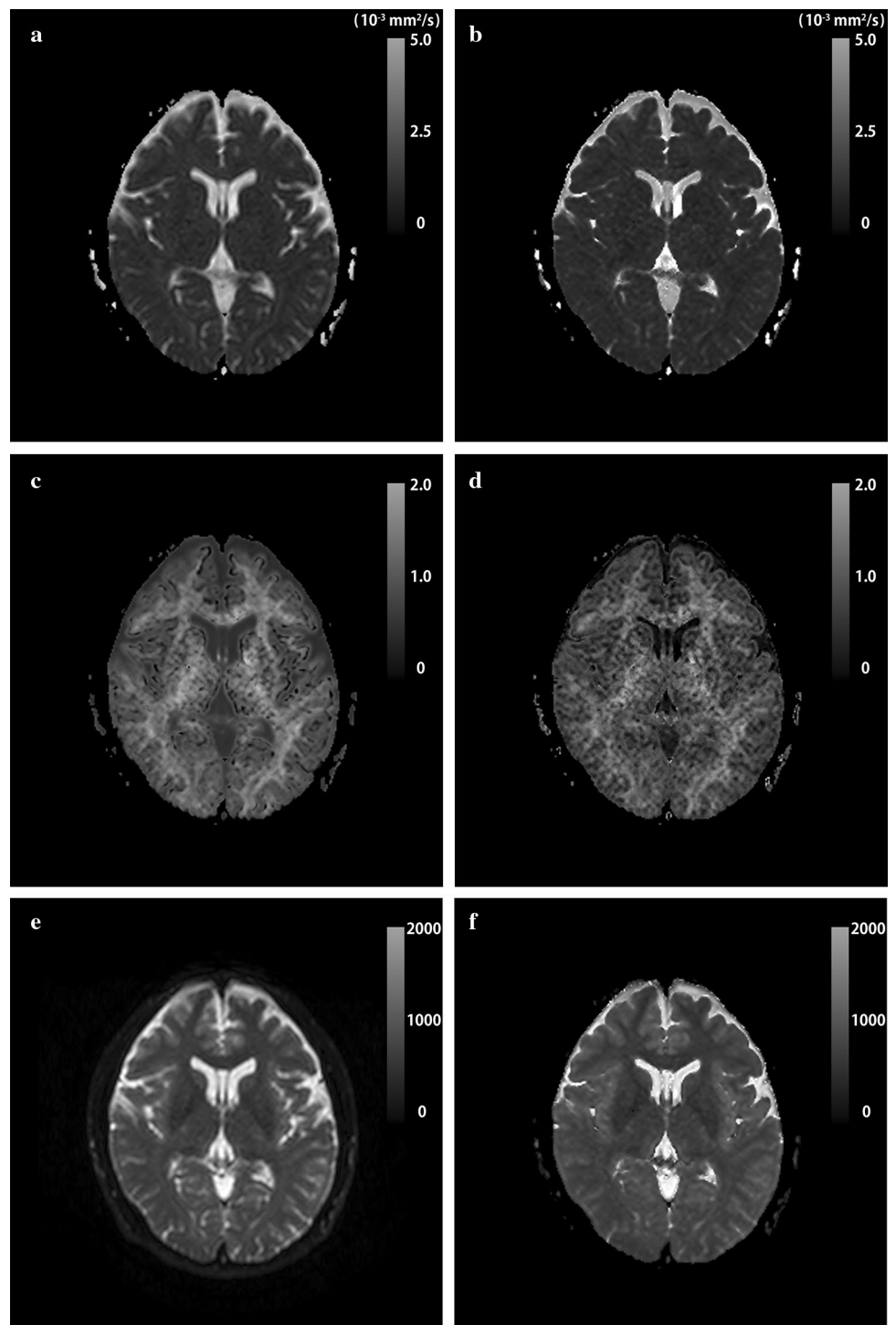


value of pure CSF is intrinsically low owing to the flow effect [13]. Moreover, the  $D$  and  $K$  values were significantly lower in the WM and GM because the data affected by tissue perfusion were not used in the second step. Le Bihan et al. reported that the  $D$  value of biological tissues is affected by varying contributions of molecular diffusion and tissue perfusion [14]. Similarly, it seems that the  $K$  values of the WM and GM were affected by the tissue perfusion.

Through a previous study, it seems that voxel-based optimization DKI is helpful in terms of improving the accuracy of the  $K$  value of biological tissues as compared to conventional DKI.

It should be noted that this study has several limitations. First, it may be difficult to evaluate whether voxel-based optimization DKI is actually helpful in terms of improving the accuracy of the  $D$  and  $K$  values, because no method to evaluate its accuracy is available. Thus, the accuracies of the  $D$  and  $K$  values had to be evaluated via comparison with values from a previous study. Second, this study analyzed a single healthy volunteer. In future studies, it will be necessary to analyze data from additional healthy volunteers to yield clinically meaningful results. Third, the image quality of voxel-based optimization DKI may be poor. This is because the number of MPG directions is low. Although the acquisition time is greater, increasing the number of MPG directions improves the image

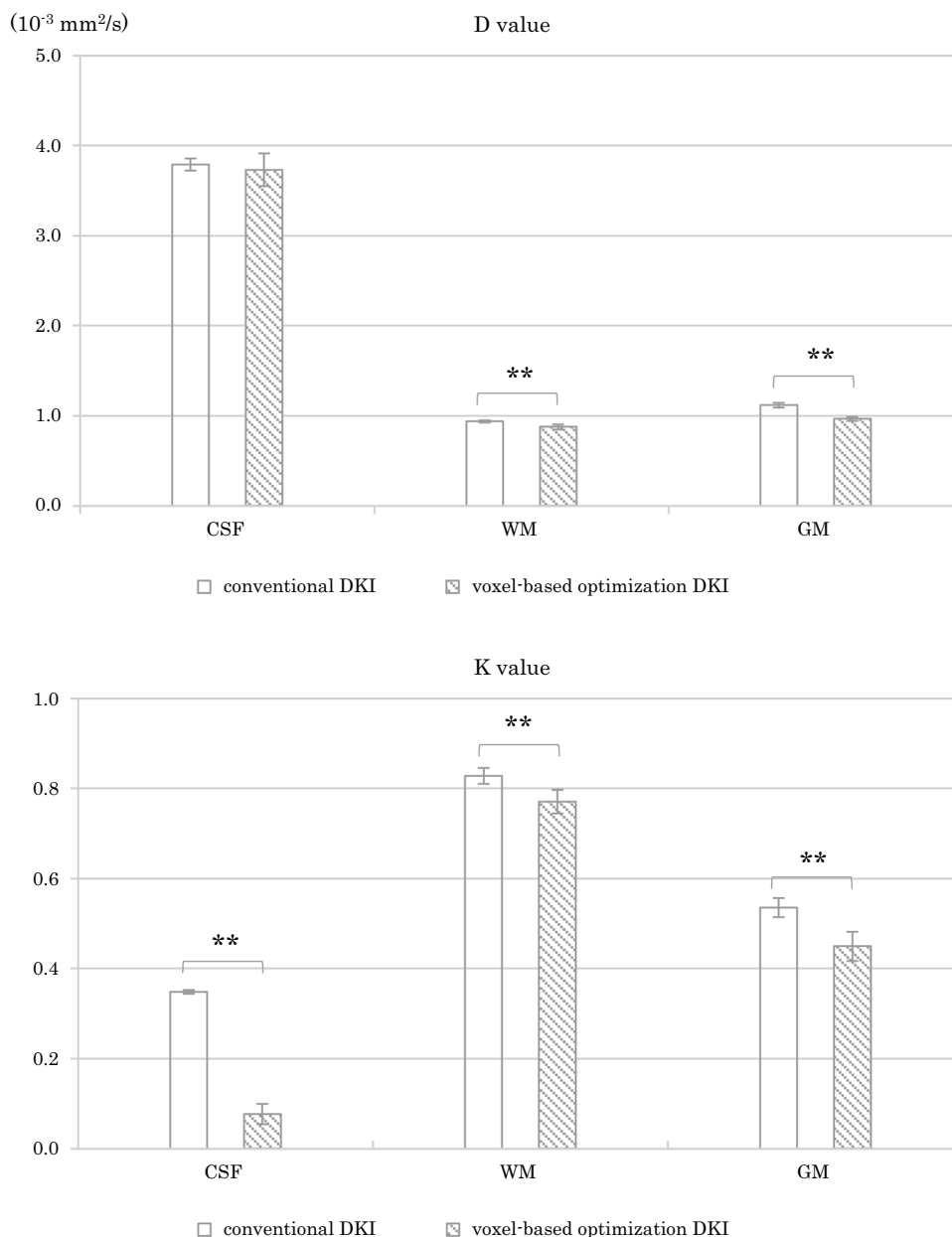
**Fig. 5** Parametric maps of  $D$  and  $K$  values in a healthy volunteer obtained using conventional and voxel-based optimization DKI: **a**  $D$  value with conventional DKI, **b**  $D$  value with voxel-based optimization DKI, **c**  $K$  value with conventional DKI, **d**  $K$  value with voxel-based optimization DKI, **e** image with  $b$  value of  $0 \text{ s/mm}^2$ , and **f**  $S_0'$  with voxel-based optimization DKI



quality (Fig. 7). Fourth, for the voxel-based optimization DKI used in this study, more images of the  $b$  values are required than in conventional DKI. Thus, the acquisition time of voxel-based optimization DKI is longer than that

of conventional DKI. However, it seems that voxel-based optimization DKI may be viable for use in brain imaging because the acquisition time determined by this study was 7 min.

**Fig. 6** Comparison of  $D$  and  $K$  values resulting from conventional and voxel-based optimization DKI in a healthy volunteer. Statistically significant differences with  $p < 0.05$  are marked with single asterisk and statistically significant differences with  $p < 0.01$  are marked with double asterisks



## 5 Conclusion

Voxel-based optimization DKI, which is used to measure the correct diffusion kurtosis by applying optimized  $b$  values for each voxel, was developed and compared with conventional DKI. Optimized  $b$  values for each voxel are needed

to measure the correct diffusion kurtosis. The voxel-based optimization DKI developed in this study is a method for optimizing the  $b$  values for each voxel, and it seems that voxel-based optimization DKI is helpful in improving the accuracy of the  $K$  value of biological tissues.

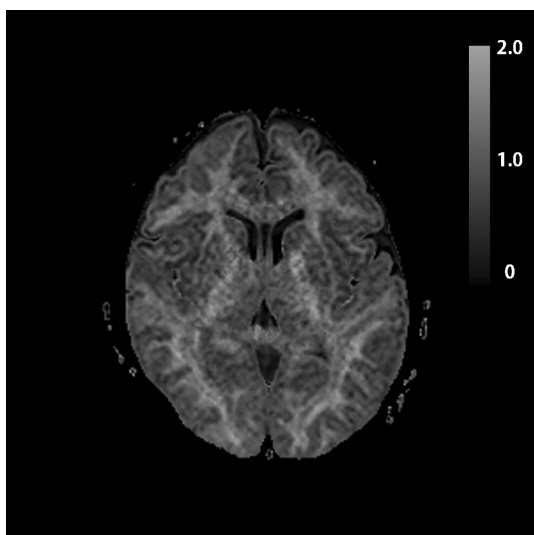


**Fig. 7** Voxel-based optimization DKI obtained using fifteen MPG directions. Although the acquisition time is longer, increasing the number of MPG directions improves image quality

**Acknowledgements** The author would like to thank Takeshi Nitanei and Tetsuya Matsumoto for their help in this study.

### Compliance with ethical standards

**Conflict of interest** The authors declare that they have no conflicts of interest.

**Statement of human and animal rights** All procedures performed in studies involving human participants were in accordance with the ethical standards of the institutional review board and with the 1964 Helsinki declaration and its later amendments or comparable ethical standards. This article does not contain any studies performed with animals.

**Informed consent** Informed consent was obtained from all participants included in the study.

### References

1. Castillo M, Smith JK, Kwock L, Wilber K. Apparent diffusion coefficients in the evaluation of high-grade cerebral gliomas. *AJNR Am J Neuroradiol.* 2001;22(1):60–4.

2. Kono K, Inoue Y, Nakayama K, Shakudo M, Morino M, Ohata K, Wakasa K, Yamada R. The role of diffusion-weighted imaging in patients with brain tumors. *AJNR Am J Neuroradiol.* 2001;22(6):1081–8.
3. Charles-Edwards EM, deSouza NM. Diffusion-weighted magnetic resonance imaging and its application to cancer. *Cancer Imaging.* 2006;6:135–43.
4. Attariwala R, Picker W. Whole body MRI: improved lesion detection and characterization with diffusion weighted techniques. *J Magn Reson Imaging.* 2013;38(2):253–68.
5. Mulkern RV, Zengingonul HP, Robertson RL, Bogner P, Zou KH, Gudbjartsson H, Guttman CR, Holtzman D, Kyriakos W, Jolesz FA, Maier SE. Multi-component apparent diffusion coefficients in human brain: relationship to spin-lattice relaxation. *Magn Reson Med.* 2000;44(2):292–300.
6. Jensen JH, Helpert JA, Ramani A, Lu H, Kaczynski K. Diffusional kurtosis imaging: the quantification of non-gaussian water diffusion by means of magnetic resonance imaging. *Magn Reson Med.* 2005;53(6):1432–40.
7. Jensen JH, Helpert JA. MRI quantification of non-Gaussian water diffusion by kurtosis analysis. *NMR Biomed.* 2010;23:698–710.
8. Fukunaga I, Hori M, Masutani Y, Hamasaki N, Sato S, Suzuki Y, Kumagai F, Kosuge M, Hoshito H, Kamagata K, Shimoji K, Nakanishi A, Aoki S, Senoo A. Effects of diffusional kurtosis imaging parameters on diffusion quantification. *Radiol Phys Technol.* 2013;6(2):343–8.
9. Wang C, Ren D, Guo Y, Xu Y, Feng Y, Zhang X, Mei Y, Chen M, Xiao X. Distribution of intravoxel incoherent motion MRI-related parameters in the brain: evidence of interhemispheric asymmetry. *Clin Radiol.* 2017;72(1):94.e1–e6.
10. Lu H, Jensen JH, Ramani A, Helpert JA. Three-dimensional characterization of non-gaussian water diffusion in humans using diffusion kurtosis imaging. *NMR Biomed.* 2006;19(2):236–47.
11. Ogura A, Koyama D, Hayashi N, Hatano I, Osakabe K, Yamaguchi N. Optimal b values for generation of computed high-b-value DW images. *AJR.* 2016;206:713–8.
12. Ogura A, Hatano I, Osakabe K, Yamaguchi N, Koyama D, Watanabe H. Importance of fractional b value for calculating apparent diffusion coefficient in DWI. *AJR.* 2016;207(6):1239–43.
13. Yang AW, Jensen JH, Hu CC, Tabesh A, Falangola MF, Helpert JA. Effect of cerebral spinal fluid suppression for diffusional kurtosis imaging. *J Magn Reson Imaging.* 2013;37(2):365–71.
14. Le Bihan D, Breton E, Lallemand D, Aubin ML, Vignaud J, Laval-Jeantet M. Separation of diffusion and perfusion in intravoxel incoherent motion MR imaging. *Radiology.* 1988;168(2):497–505.

**Publisher's Note** Springer Nature remains neutral with regard to jurisdictional claims in published maps and institutional affiliations.